# Design and Analysis of an Aircraft Wing

**Ryan Miguel Gonzales, Alexander Liou, Anthony Matimu, Chris Beloglazov, Karim Elyoussef**
*Department of Mechanical and Aerospace Engineering, Princeton University, Princeton, NJ 08544 USA*
Prepared for MAE 321 Engineering Design Final Project on December 1st, 2023

**With the use of design and analysis tools, the group aimed to produce the lightest aircraft wing possible capable of withstanding a load of 90 lbs applied on the wing tip. A provided tutorial was used to create the initial I-beam, bulkheads, and surface. Subsequently, the group considered the material, structure of the I-beam web, and balance between weight, tensile strength, and deflection to transform the initial design. The final version of the wing spar was designed and optimized through multiple iterations using innovative features to strike a balance between characteristics in consideration.**

**The wing was machined from a stock bar of aluminum with dimensions 36” x 1” x 0.75”. Simulations performed on the I-beam concluded that 7075 T6 Aluminum meets load requirements while minimizing weight. Ultimately, the stress in the wing was designed to fall under the yield stress of the material, with a minimal safety factor implemented due to the inherent strength of additional components appended to the final assembly, including an aluminum skin, bulkheads, and rivets.**

**In testing, the wing was found to be the lightest in the class and successfully carried a load of 90 lbs with no plastic deformation, eventually fracturing at 180 lbs. Fracture and shearing occurred as expected from the simulation, while the actual deflection was less than expected.**

## Table of Contents

## Introduction

In the design of an aircraft wing, there are several important considerations, including load bearing, strength, weight, and deflection. A wing should be able to hold a given amount of weight without permanent deformation or fracture, and be light to allow the aircraft to safely perform takeoff, landing, and other actions. In a situation where the wing is to be used repeatedly, the wing should be relatively easy to maintain and inspect for damages. Additionally, the wing must be able to generate enough lift to allow the aircraft to fly with a reasonable amount of weight and load.

The goal of this project was to design and construct an airfoil wing capable of withstanding a 90lb load applied to the wing tip. The assignment allowed for the design of the wing spar or beam to be modified as needed within given constraints (e.g. length) and with changes made to the bulkheads of the wing to accommodate. Other aspects of the wing such as the symmetrical aerofoil shape and bulkhead material were provided and could not be modified. This wing was planned to only be used once, meaning that maintenance and upkeep were not of importance. Considerations of fatigue and implementation of S-N curve theory were not applicable since the wing would only experience a few cycles of different weights until it yields.

Material selection was limited to those available through McMaster-Carr. In choosing the material, the top factors were tensile strength and density. Aluminum 7075 alloy, which is commonly used in the aerospace industry, was chosen as the manufacturing material for its high tensile strength compared to other alloys (see Appendix D) and low weight compared to steel. T6 temper 7075 has an ultimate tensile strength of 62.9–84.1 ksi and yield strength of 52.1–76.9 ksi. With this material consideration, our spar was designed to experience stresses mostly below the midpoint of this yield strength range, around 59 ksi.

Though cost was a slight factor in our selection of material, it was not the most pressing constraint. Thus, we decided to trade cost for strength, picking the most costly material of our four considerations in order to have a material with the highest tensile strength.

Mechanical properties of T6-7075 aluminum can be found in Appendix A and properties of the stock material purchased from McMaster-Carr can be found in Appendix B. A cost chart of options considered can be found in Appendix C.

Testing was conducted by attaching a series of increasing loads on the end of the wing, measuring deflection with each load, until the beam fractured. The wing was considered to be successful if it passed the 90 lb load without fracture and was the lightest wing of the four groups in the class.

# Background

## Specifications

While many changes can be made regarding the design of the beam, several specifications must be met. The aforementioned load of 90 lbs is the sole determining factor for the success of the beam. The total length of the beam is 25.5", while the load at the end is 23.5" from the nearest support. The beam must also conform to a mounting fixture for machining and a mounting apparatus for load testing which has dimensions of 0.75" x 0.75" (see Appendix F). Data from CES 2019 EduPack provided a wide variety of figures for material selection; namely, yield strength and density.

## Theory

The majority of our concern lay in the stresses induced as a result of bending, the maximum of which can be described by the equation

$$\sigma = \frac{My}{I}$$

where "y" is the largest distance from the centroid in the upward transverse direction, and "I" is the moment of inertia. Given that our beam's height was constrained to be 1 in, our focus was on increasing the moment of inertia of the I-beam to reduce stress. In general, the moment of inertia of an I-beam can be calculated as follows:

$$I = \frac{A^3B}{12} - \frac{a^3b}{6}$$

where "A" is the outside cross-section height, "B" is the outside width, "a" is the distance between the flanges, and "b" is the minimum perpendicular distance from the web to the outermost edge of the flange. Part of our focus was thus to minimize values "a" and "b" while maintaining a lightweight for the wing.

While a consideration, shear stress was a negligible failure theory consideration, as it produced independent stresses that were much less than those created by bending normal stresses. Via rapid hand calculations, shear stresses were generally less than 5% of the maximum yield stress of 7075 alloys. Considering that shear strength is generally accepted to be less than (approximately ¾) of yield strength, the limit was still far from being reached as a result of pure shear.

# Theoretical Design Analysis

Structural analysis was conducted using PTC Creo's Simulate application. The wing structure was simulated using full constraints on the fixed end (the end with the larger cross section) of the wing and a 90 lb force downwards on the free end of the wing (see Appendix E). The final product was machined using a CNC milling machine using PTC Creo to generate the GCode program. As both sides of the workpiece need to be machined, a special apparatus with five holes was required to secure and keep the workpiece aligned and mounted for both machining phases (see Appendix F). This was properly accounted for when designing, simulating, and milling the beam.

Additionally, the beam required manual milling before CNC milling. The stock was cut to 25.5” from the original 36” to match the milling volume defined in Creo. The other dimensions required no manual milling and could be used directly for the milling volume in Creo (1” by ¾”). The direct use was due to the specified coordinate system origin being placed in the middle of the 1” segment; this meant that the wing was cut symmetrically from a central axis spanning the length of the beam, allowing the group not to worry about any imperfections in the factory ends.

## Procedure

During the initial design of the wing, a tutorial was followed to create a central I-beam, wing ribs bulkheads, and a wing surface. For the design project, the wing I-beam was redesigned separately. At first, a beam similar to the tutorial beam was configured to have higher rigidity and lower weight than the tutorial beam. However, we quickly realized that stress concentrated in the center of the beam was a limiting factor to our design. Thus, we changed our design to minimize stress near the center while maintaining a lightweight.

We used a novel three-cross-section design (placed at both ends and the center) to make a nonlinear taper that kept the I-beam tall in the center to increase its moment of inertia and decrease stress in the center. This also enabled very thin material to be used, lightening the beam further. The beam was simulated with a 90 lb vertical cantilever load over a dozen times to optimize dimensions and lightning patterns, and an additional 5 lb load was added horizontally to attempt to account for potential twists in the beam.

Ultimately, our goal was to remain below 59 ksi stress in most regions, with peaks up to 70 ksi in corners of stress concentration. Adjusting dimensions and radii allowed us to decrease the concentrated stress at some points. The final result is pictured as follows:

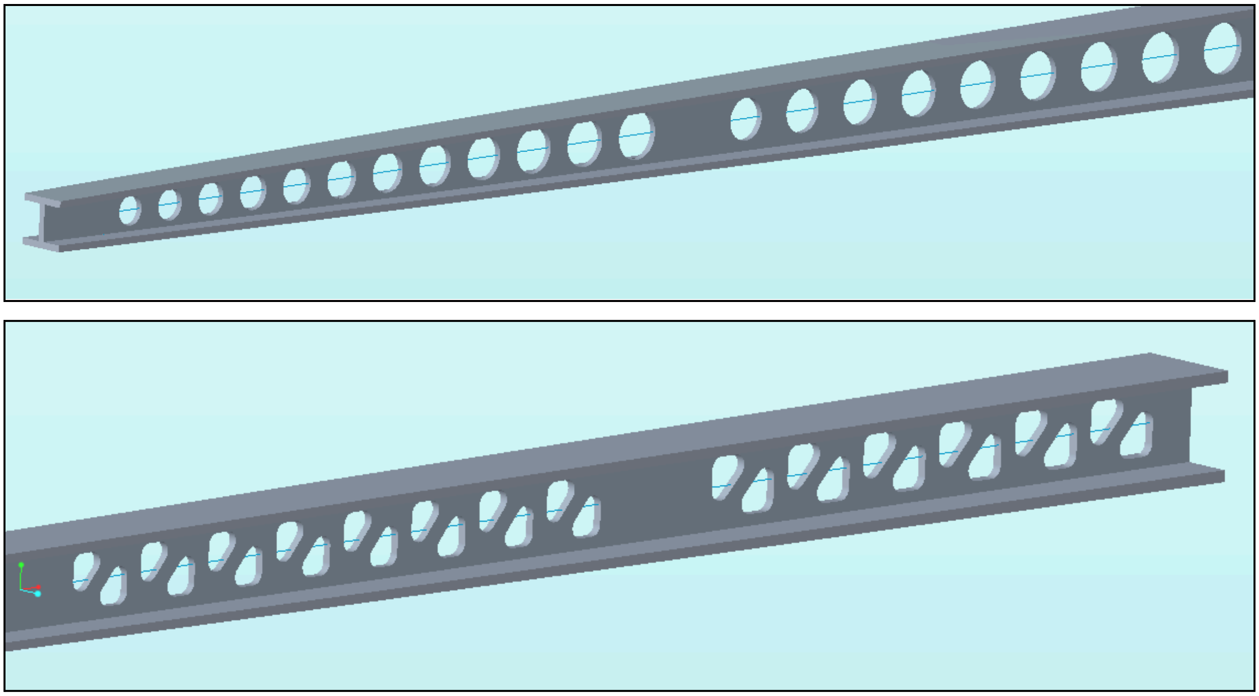

Figure 1: Lightening pattern of circles near the narrow end and triangular truss near the thicker end. These patterns were chosen for the high strength-to-weight ratio of trusses and the set minimum radii of the tool.

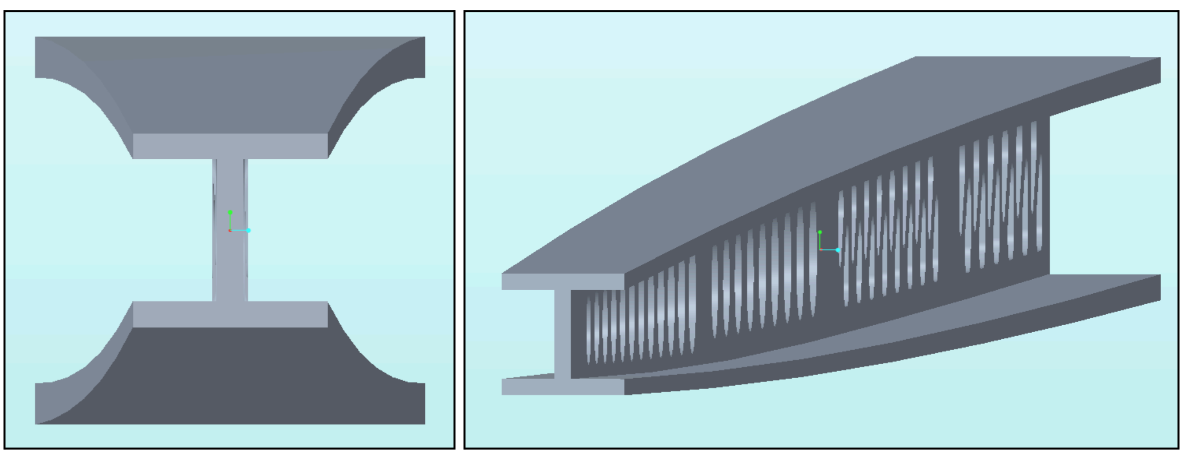

Figure 2: The nonlinear taper of the beam can be seen from the front and corner view. Note that the flange and web thicknesses also vary nonlinearly along the longitudinal direction of the beam.

Static analyses were performed in various configurations on each iteration of the beam. A tradeoff was made between deflection, weight, and maximum stress, prompting a thoughtful balancing act in design and iteration. Key values are listed in Table 1 from the simulation results:

| | |
|---|---|
| Predicted Maximum Realistic Stress | 66 ksi |
| Predicted Deflection | 3.9 in |
| Predicted Volume | 3.576 in^3 |
| Predicted Weight (spar only) | 0.3647 lbs |
| Predicted Total Weight | 1.1 lbs |

Table 1: Key Values of I-Beam

Simulations showed that stresses were well-spread across nearly the entire length of the beam as intended with our nonlinear cross-section design, as viewed in Figure 3. Skin stress for most of the beam generally remained between 50 and 59 ksi, well within the upper limit of the yield stress range of 7075 alloys. As seen in Figure 5, the deflection was predicted to be around 3.9 inches.

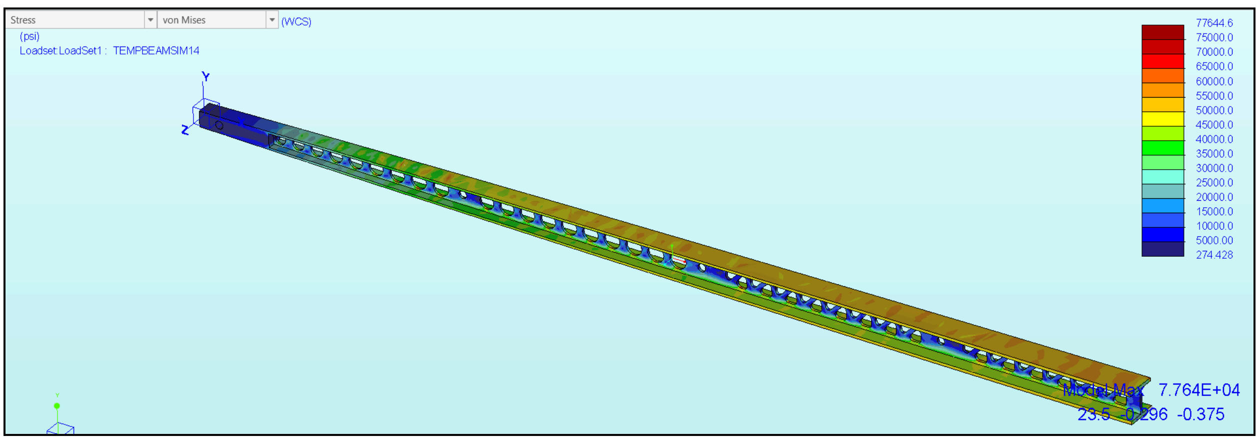


Figure 3: Beam stress profile. Note that the maximum stress is fictitious at the corner of the end mounted to the fixture. Note that stress is well-distributed along the top and bottom flanges, as we used a nonlinear taper to alleviate stresses concentrated in the center.

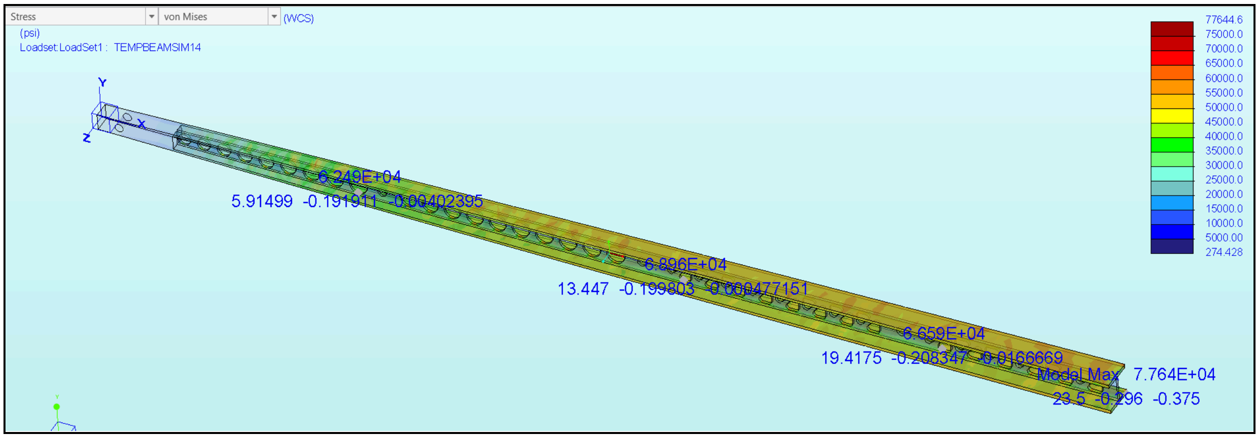


Figure 4: Beam stress profile with selected regions highlighted as high-stress points. These are generally focused in the lightning pattern areas where large moments are experienced.

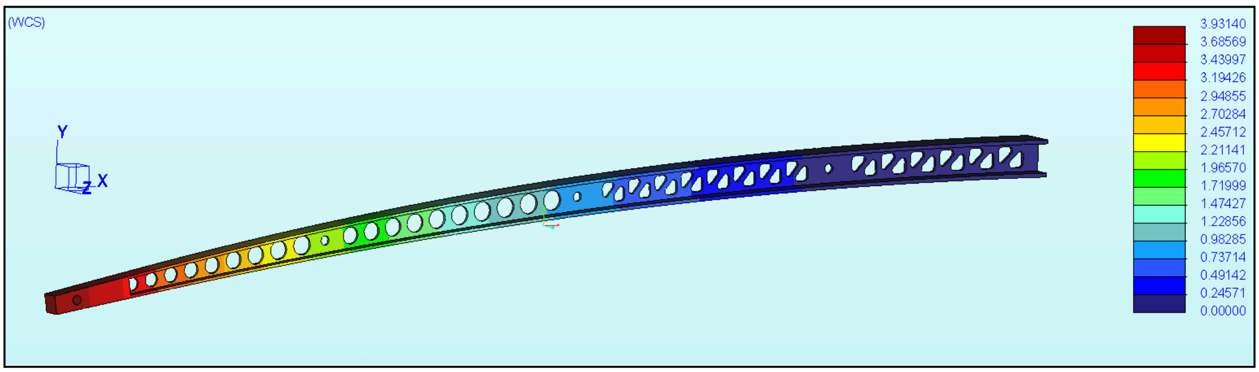


Figure 5: Deflection profile showing a maximum theoretical deflection of 3.9 inches.

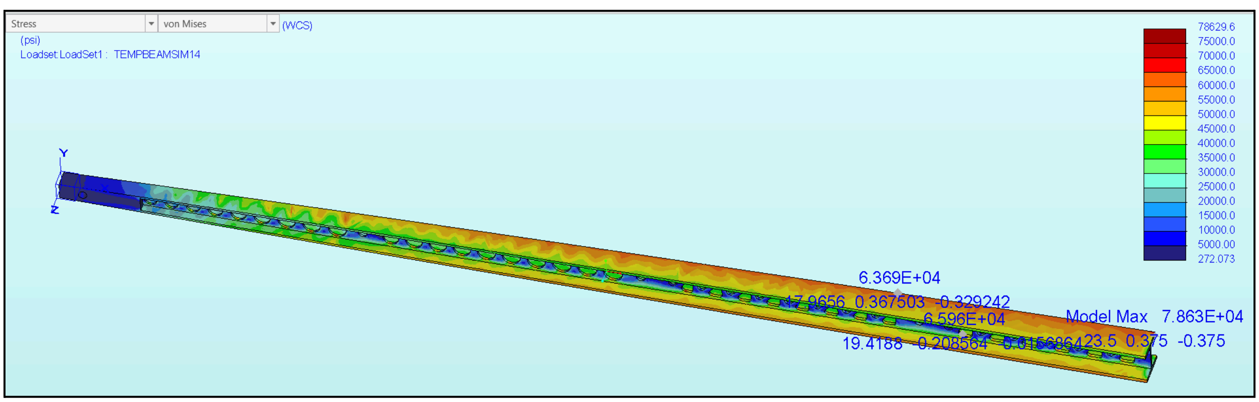


Figure 6: When under a 90 lb vertical load and 5 lb horizontal load, stresses shift to the side and rise slightly.

The fully assembled wing is shown in Figure 7. First, our 7075 aluminum stock was milled to size using a manual mill and jig. Holes were drilled and counterbored to mount the stock to the CNC mill during milling. Two milling operations were performed on the beam, and it was post-processed to remove additional protrusions and fit into the fixture. Two aluminum end bulkheads and seven 3D-printed PLA intermediate bulkheads were riveted to the beam using ⅛” aluminum rivets. Figure 8 shows the rig used to prepare the stock.

Rivets were applied on the bottom of the assembly in order to maintain the continuity of material under tension on the top of the beam. Since the bottom of the beam would be under compression during loading, the rivets would be compressed and offer some resistance to deformation. PLA leading edges were riveted to the bulkheads. The skin of the wing was cut from 0.02” aluminum sheet and pre-bent. The skin was riveted to the bulkheads of the wing and provided a safety factor to the loaded wing. Since the top aluminum sheet experienced high tensile loads, seven rivets were used to mount it to the fixed support bulkhead.


Figure 7: The fully assembled wing with bulkheads, skin, and beam.

Figure 8: Manual milling rig used to prepare the stock for CNC machining.

## Individual Contributions

Table 1 below lists the contributions of each group member to the overall project, filling corresponding boxes with green for each task that they assisted with.

| Name | Ryan | Alex | Karim | Chris | Anthony |
|---|---|---|---|---|---|
| Final Assembly | | | | | |
| CNC Milling | | | | | |
| Material Selection | | | | | |
| Manual Milling | | | | | |
| CAM Encoding | | | | | |
| Simulation and Analysis | | | | | |
| Initial Design | | | | | |
| Optimization and Weight Reduction | | | | | |
| Drawings and Figures | | | | | |
| Report Writeup | | | | | |

## Conclusion

The results of the simulation showed that the beam would be able to withstand the required amount of 90 lbs, as the maximum stress experienced by the beam was on the lower end of the tensile stress range of 7075 Aluminum. Calculations for the weight of the beam provided favorable results, showing that the beam alone will weigh around 0.365 lbs, which was relatively lightweight for this task.

The beam was designed with little safety factor due to the real-life structural contributions of additional components that will add to the strength of the beam. Additionally, the beam was designed for single use and thus did not focus on ease of repair, long-term maintainability, or fatigue cycle concerns. The additional structure provided by the sheet metal exterior, rivets, and bulkheads was expected to increase the overall strength and weight of the structure. These extra additions to the I-beam may have had some significant effects on the performance of the wing, which was monitored throughout the testing phase.

The testing phase consisted of placing six different loads (measured in lbs) on the end of the beam: 65, 90, 115, 140, 165, and 180. The apparatus is pictured below in Figure 9. The beam was considered to have passed testing if it could hold the 90 lb load without fracture. Deflection at the end of the beam was measured after each load.

Before testing, our beam was weighed in at 1 lb, 3.9 oz, making it the lightest wing of the four in the class by a minimum difference of 0.1 oz. Our beam passed testing with a measured deflection of 3.25” for the 90 lb load; this was slightly less than our expected deflection of 3.9” from simulations. As loads increased, the beam began to plastically deform, ultimately fracturing at the top of the beam while lifting the 180 lb load. Shearing was noticed on the top rivets that attached the skin to the aluminum bulkhead, and significant bending was noted on the underside of the wing.

Ultimately, the beam deflection was relatively consistent with what the simulations predicted, with bending being distributed along the length of the beam. The beam fractured near the fixed support, which is consistent with the fact that the moment at the fixed support is largest and thus produces the highest normal stresses. Since aluminum is a ductile material, it first began to neck and finally fractured in the direction of the highest shear stresses, which arise from normal stresses when the coordinate system is rotated by 45 degrees. Figure 10 shows the fracture profile in detail, including the necking characteristics and fracture angle. Tensile stresses reached a yield criterion first, as the beam did not buckle significantly. Figure 11 shows the rivets shearing the aluminum skin under a 165 lb load.


Figure 9: A load test of 140 lbs is applied to the end of the cantilevered beam via a winch system. The beam was fixed to the back of a manual mill.

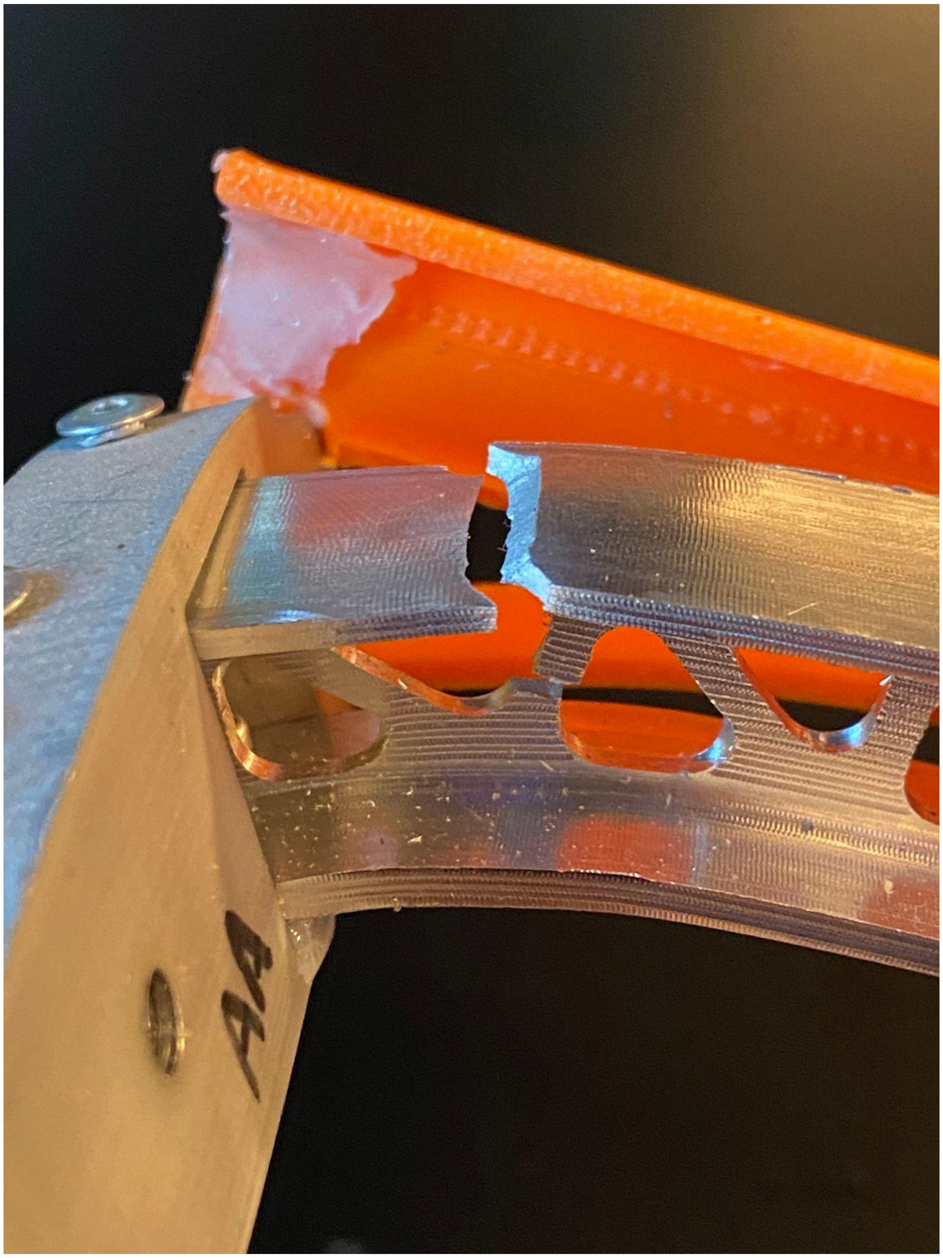


Figure 10: Fracture profile of the beam near the fixed support.


Figure 11: The rivets mounting the skin to the fixed bulkhead sheared the skin under a 165 lb load.

# Appendix

Appendix A: Material properties of Aluminum, 7075, T6

| **Property** | **Min** | **Max** | **Unit** |
|---|---|---|---|
| **Young's modulus** | 10 | 11 | $10^6$ psi |
| **Specific stiffness** | 8.23e6 | 9.1e6 | lbf.ft/lb |
| **Yield strength (elastic limit)** | 52.1 | 76.9 | ksi |
| **Tensile strength** | 62.9 | 84.1 | ksi |
| **Specific strength** | 4.28e4 | 6.32e4 | lbf.ft/lb |
| **Elongation** | 2 | 10 | % strain |
| **Compressive strength** | 57 | 76.9 | ksi |
| **Flexural modulus** | 76.9 | 11 | $10^6$ psi |
| **Flexural strength** | 52.1 | 76.9 | ksi |
| **Shear modulus** | 3.77 | 4.06 | $10^6$ psi |
| **Bulk modulus** | 9.72 | 10.7 | $10^6$ psi |
| **Poisson's ratio** | 0.325 | 0.335 | |
| **Shape factor** | 16 | | |
| **Hardness - Vickers** | 152 | 168 | HV |
| **Hardness - Brinell** | 145 | 165 | HB |
| **Elastic stored energy (springs)** | 11.1 | 22.7 | ft.lbf/in$^3$ |
| **Fatigue strength at $10^7$ cycles** | 22 | 24.4 | ksi |
| **Fatigue strength model (stress range)** | 17.5 | 30.6 | ksi |

*Data from Ansys CES 2019 Edupack*

Appendix B: Stock Material Properties

| **Property** | **Value** | **Units** |
|---|---|---|
| **Price** | 98.05 | USD |
| **Thickness tolerance** | ± 0.003 | in |
| **Width tolerance** | ± 0.010 | in |
| **Specification** | ASTM B211, SAE AMS-QQ-A-225/9 | |

*Data from McMaster-Carr*

Appendix C: Comparison of Aluminum Costs

| **Aluminum Alloy** | **Cost, USD (Stock: 36 in x 1 in x 0.75 in)** |
|---|---|
| AL2024 | $85.27 |
| AL6013 | $81.19 |
| AL6061 | $27.11 |
| AL7075 (Selected) | $98.05 |

*Data from McMaster-Carr*

Appendix D: Comparison of Aluminum Densities and Tensile Strengths

| **Aluminum Alloy** | **Max Tensile Strength, psi** | **Max Density, $lb/in^3$** |
|---|---|---|
| AL2024 | 74000 | 0.101 |
| AL6013 | 61800 | 0.0987 |
| AL6061 | 49000 | 0.0987 |
| AL7075 | 80100 | 0.102 |

*Data from Ansys CES 2019 Edupack*

Appendix E: Wing Assembly and Aerofoil Shape

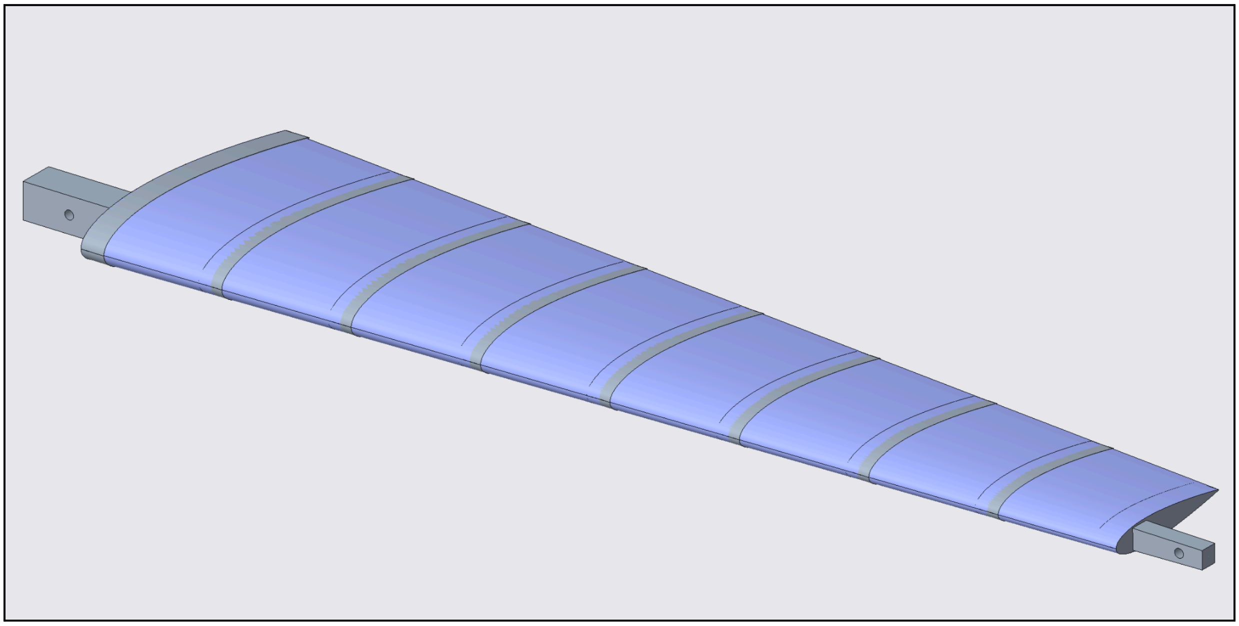

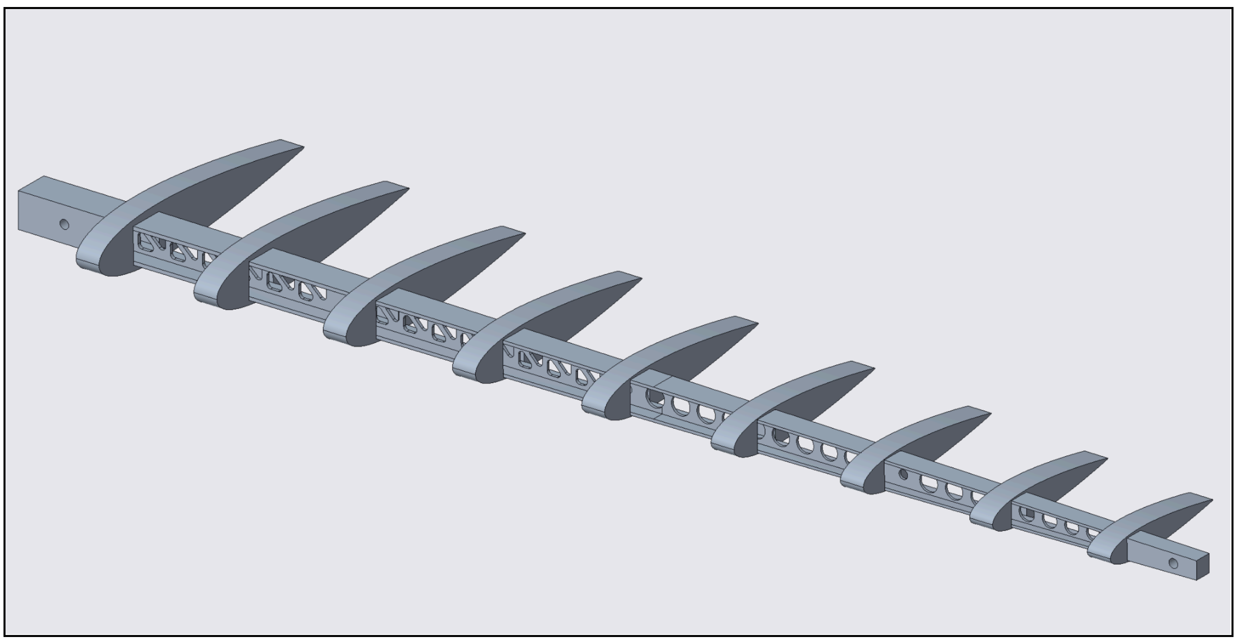

Appendix F: Gallery of Testing Phase and Final Assembly

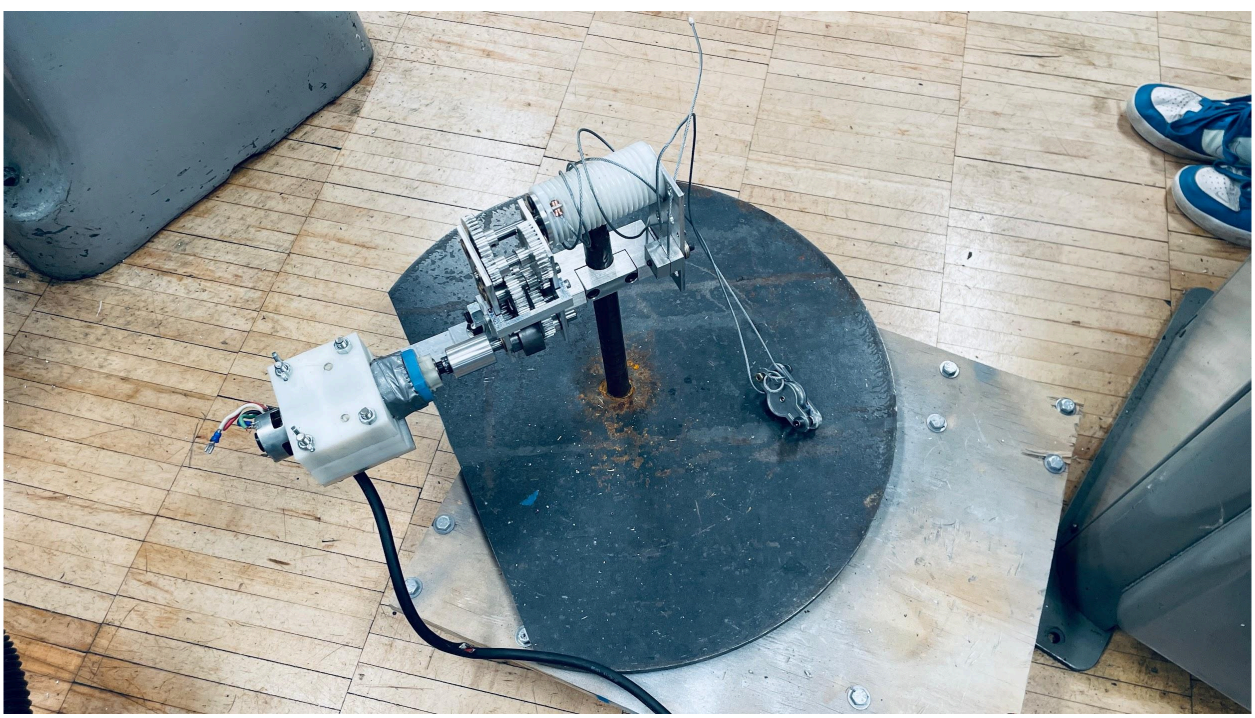


DECIMAL EQUIVALENTS


Appendix G: Engineering Drawings (next page)

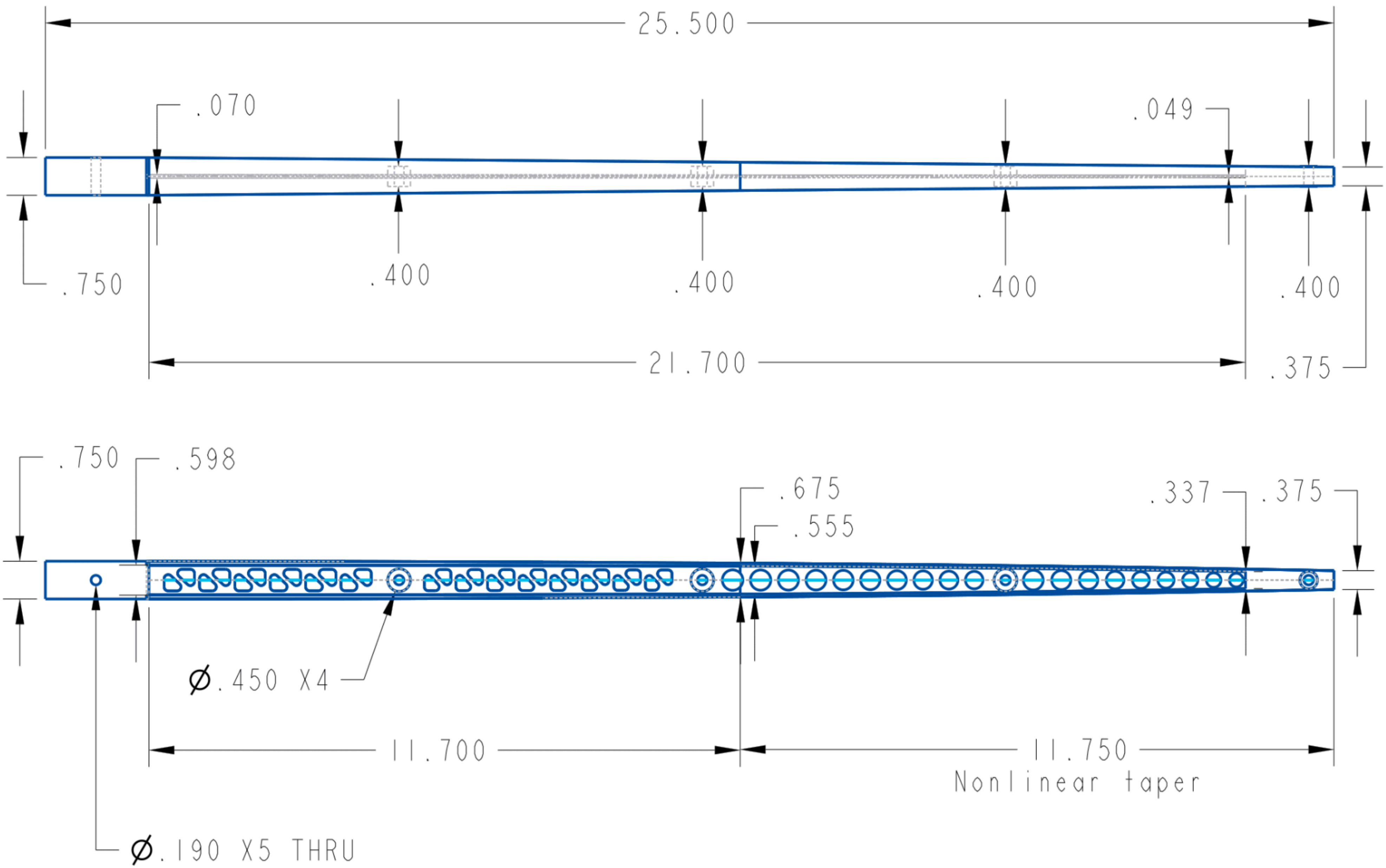


SCALE 0.400

Tolerance ± 0.005 for all dimensions

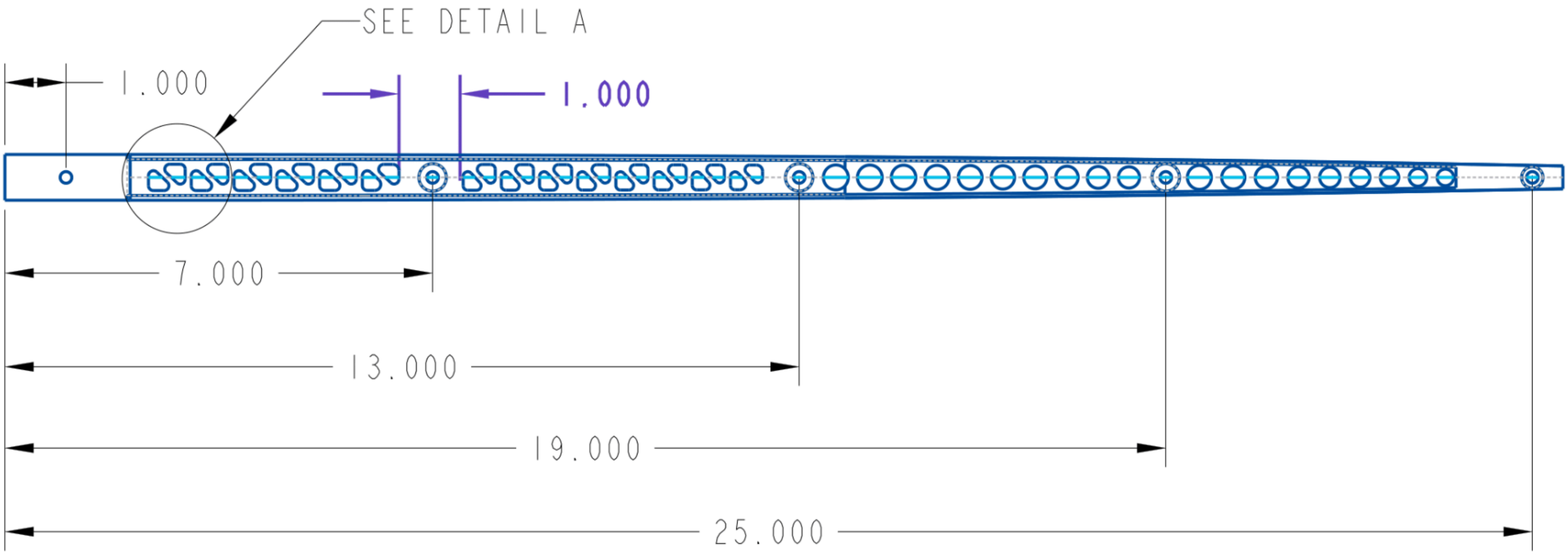


DETAIL A
SCALE 1.500
Dimensions not
typical for truss

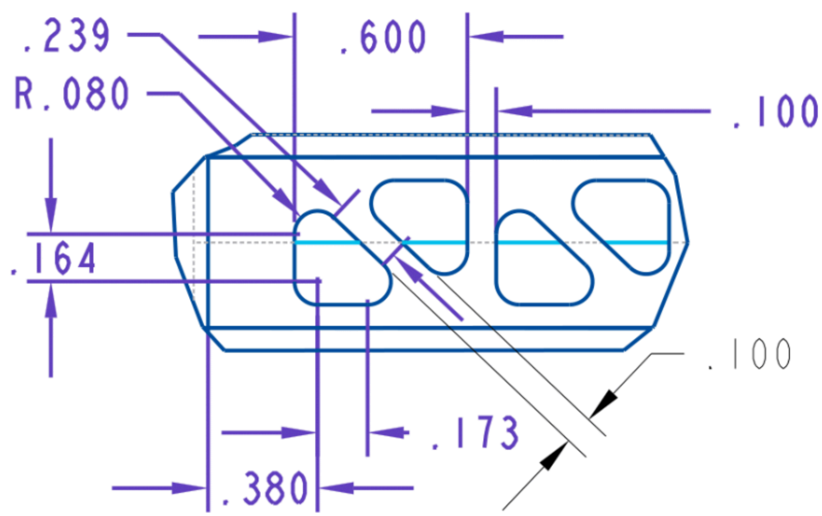


SCALE 0.400

Tolerance ± 0.005 for all dimensions


SCALE 0.625

| HOLE | FROM X | DIAMETER |
|---|---|---|
| A | 13.550 | 0.406 |
| B | 14.104 | 0.403 |
| C | 14.655 | 0.399 |
| D | 15.202 | 0.394 |
| E | 15.742 | 0.388 |
| F | 16.277 | 0.381 |
| G | 16.804 | 0.374 |
| H | 17.324 | 0.365 |
| I | 17.835 | 0.357 |
| J | 18.337 | 0.347 |
| K | 19.500 | 0.392 |
| L | 20.055 | 0.378 |
| M | 20.596 | 0.364 |
| N | 21.123 | 0.350 |
| O | 21.636 | 0.335 |
| P | 22.132 | 0.319 |
| Q | 22.614 | 0.304 |
| R | 23.080 | 0.288 |
| S | 23.530 | 0.272 |

SCALE 0.400

Tolerance ± 0.005 for all dimensions

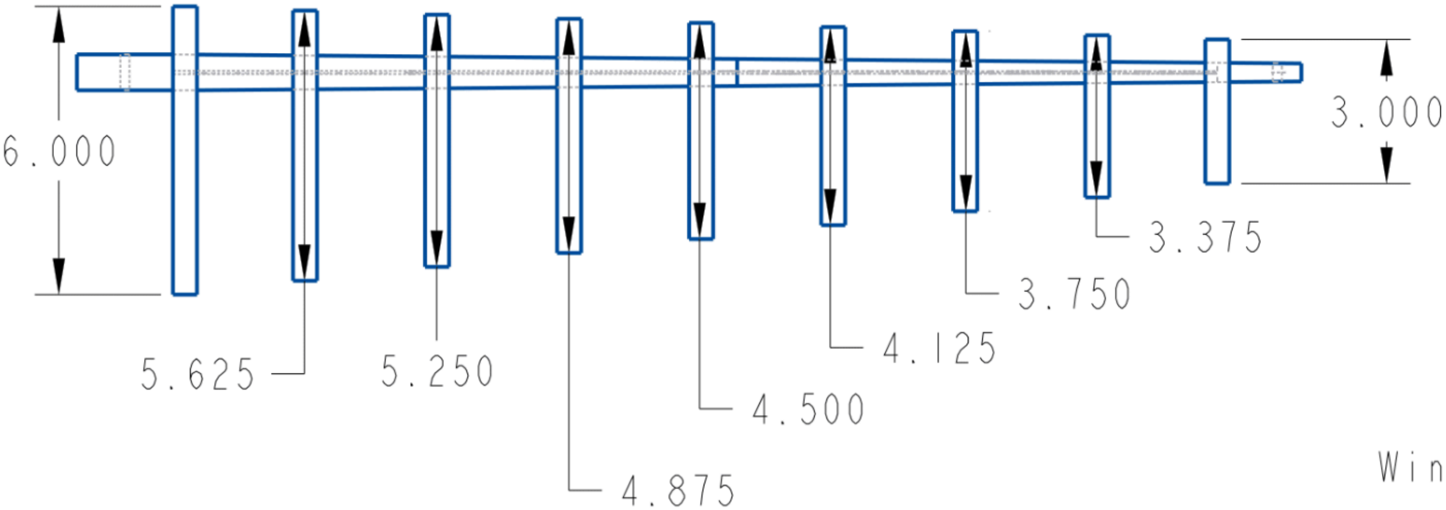


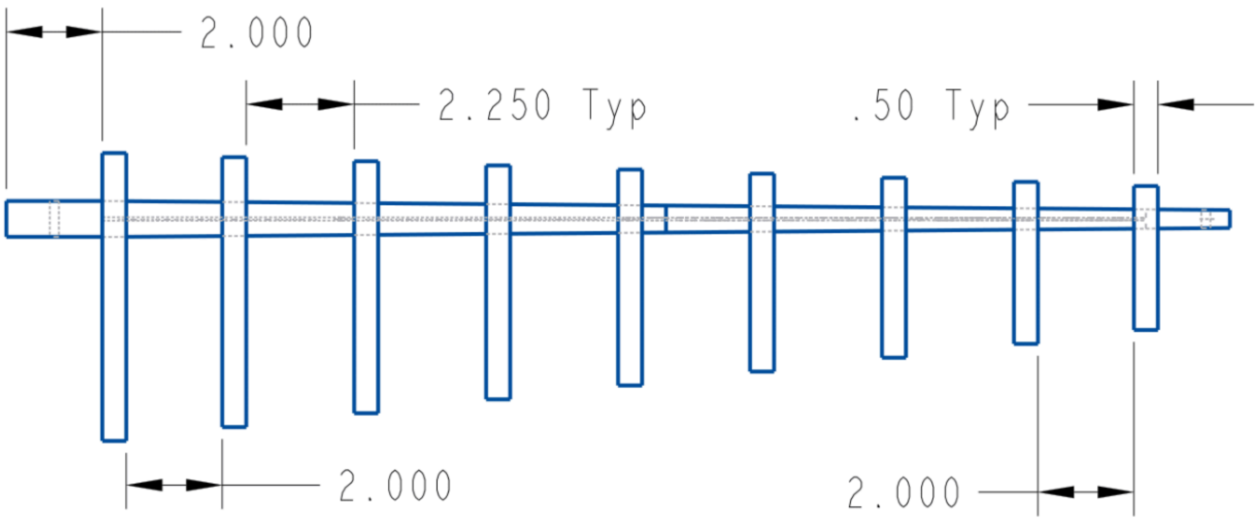


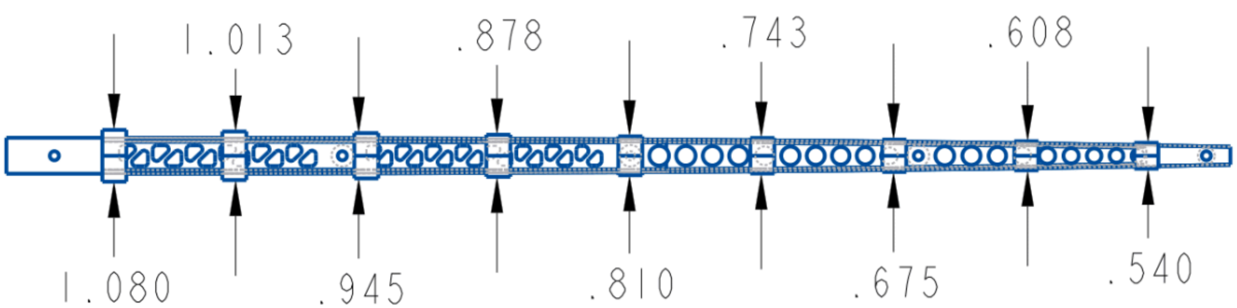


Wing Assembly

Bulkhead square cutout
for beam is nonlinear

Tolerance ±0.005
for all dimensions

SHEET 1 of 2

SCALE 0.250

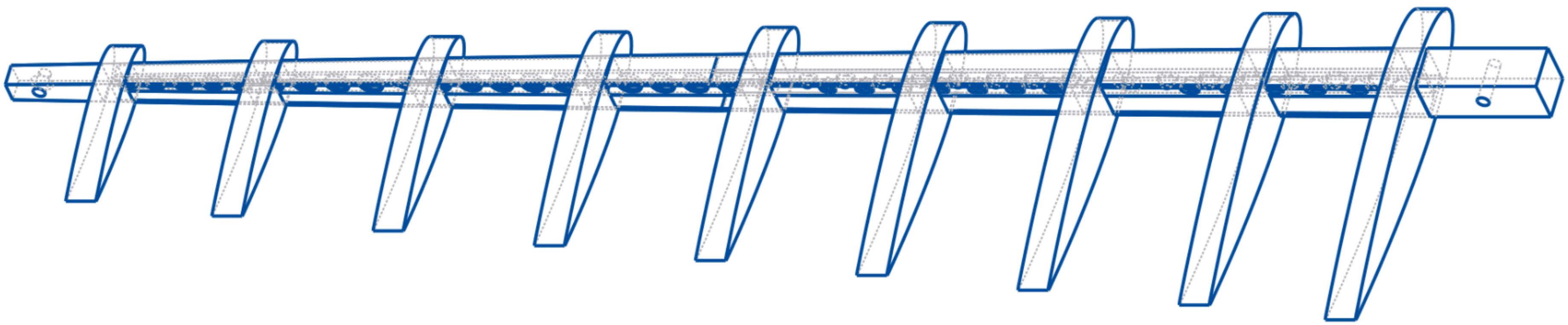

SCALE 0.400